Gain-Scheduled Steering Control for Autonomous Vehicles

Dimitrios Kapsalis, Olivier Sename, Vicente Milanés, John Jairo Martinez Molina

Gain-Scheduled Steering Control for Autonomous Vehicles

Dimitrios Kapsalis[1,2], Olivier Sename[2], Vicente Milanes [1] and John J. Martinez[2]

***Abstract*— This paper presents an Linear Parameter Varying (LPV) approach for the lateral control of autonomous vehicles, in order to take into account the whole operating domain of longitudinal speeds, as well as the variation of the look-ahead distance. Combining a dynamical vehicle model with look-ahead dynamics, together with an identified actuator model including an input delay, the closed-loop performances can be achieved and the tracking capabilities can be improved for every speed. This is obtained in particular through *ad hoc* representation of the look-ahead time as a parameter-dependent function. An H_∞/LPV control problem is formulated considering parameter-dependent weighting functions, allowing the control adaptation for all speeds. The synthesis is performed using the gridding approach, in order to account for varying parameter rate. The proposed steering control system has been implemented on a real electric Renault Zoe car. The performances are therefore assessed experimentally on a real test track with a varying longitudinal speed profile, and compared with a classical LPV polytopic controller, which proves the advanced lane-tracking capabilities of the proposed methodology.**

I. INTRODUCTION

Automated vehicles will enhance road safety, increase highway capacity, reduce carbon emission, and make transportation more accessible to disable and older people. But they are complex systems since engineers have to take into account multi-parametric requirements, such as vehicle and passenger safety, fuel and power economy and efficient driving [1].

Intelligent vehicles' architecture is at the intersection of multiple research fields ranging from location or perception to path planning and control [2]. Among them the control architecture can be classified into different categories according to the considered dynamics (and degrees of freedom) such as: Lateral control, Longitudinal control, Integrated Lateral/Longitudinal control and higher control issues [3].

Lateral control refers to as the ability of automatically steer a vehicle, and perform maneuver such as lane changes. If lateral control can be tackled using several actuators, as active front steering with an additional yaw moment (see [4] for a nonlinear MPC method and [5] for an H_∞/LPV one) it is still of high interest to deal with the steering control only.

Major contributions have been achieved the previous decades on the steering control for autonomous vehicles. Ackermann [6] was one of the first that made a breakthrough on lateral control by applying active steering with yaw rate error compensation to decouple the yaw and lateral dynamics. In 1995, Carnegie Mellon University demonstrated the Navlab car [7] completing a cross-country journey, whose steering control minimized the lateral deviation of the vehicle and its heading error. In 1998, Broggi [8] leading the ARGO project, performed a journey through Italy in autonomous mode and its control implementation was based on a variable gain proportional controller minimizing a lateral offset at a look-ahead distance according to the reference trajectory. In 2005, Stanley vehicle [9] won the second DARPA Grand Challenge whose steering action was a non-linear function of the cross-track error and the vehicle's orientation error, measured relatively to the nearest path segment. In [10], the authors demonstrated in the Grand Cooperative Driving Challenge of 2016 a driverless electric vehicle whose control system was a state feedback with pole placement using the kinematic bicycle model of the vehicle, minimizing the cross-track and heading errors of the vehicle.

More recently, various control techniques have been successfully applied for lateral control. To cite a few, in [11], Model Predictive Control (MPC) approaches were formulated using a non-linear model in the first case and in the second an on-line linearization vehicle model, solving a finite horizon optimal control problem respecting the state constraints for the stabilization of the car. [12] proposes a preview steering control design that tackles communication delay, steering lag and is implemented as a state feedback controller that uses as a feedforward term the future road curvature information. In AUTOPIA program different steering systems were implemented in mass-produced cars focused on fuzzy logic: A cascade control architecture [13] was implemented mimicking a human driver's behaviour and in [14] genetic algorithms were used to adjust automatically a fuzzy steering controller. Moreover, fuzzy logic was used in [15], where they demonstrated a constrained Takagi-Sugeno control method using fuzzy Lyapunov control framework for automatic lane keeping. In [16], a PID controller was proposed as a model of how drivers steer based on observations and was validated on a bus revenue service. The output of the controller is the rate of the steering angle with a single gain that minimizes desired and current yaw rate values.

On the other hand, to deal with complex non-linear systems, gain-scheduling control is a key design procedure which arises in many applications. Indeed LPV control theory emerged to handle robustness and performance guarantees for the whole operating domain of the varying parameters of dynamical system [17]. Let us mention that

*This work was supported by Renault.

[1]Dimirios Kapsalis and Vicente Milanes are with the Research Department, Renault SAS, 1 Avenue de Golf, 78280 Guyancourt, France dimitrios.kapsalis@renault.com vicente.milanes@renault.com

[2]Dimitrios Kapsalis, John Jairo Martinez Molina and Olivier Sename are with GIPSA-lab, Control Systems Department, 38000 Grenoble, France dimitrios.kapsalis@grenoble-inp.fr john-jairo.martinez-molina@grenoble-inp.fr olivier.sename@grenoble-inp.fr

LPV gain-scheduling control has been successfully applied to the control synthesis for many aerospace applications as in the problem of active flutter suppression [18] but also in the automotive sector. Thus this approach has shown its value for various complex intelligent vehicle applications [19], such as global chassis control, semi-active suspension control [20], or active anti-roll bar system of heavy vehicles [21]. See [22] for an interesting survey of LPV applications.

However, as far as our knowledge is concerned, its potential with regard to autonomous vehicles has so far been very little explored. As illustration, LPV theory has been used for automatic lane keeping in [23], where a grid-based approach is used to synthesize LPV controller which is implemented and tested on a tractor-trailer. The velocity-dependent controller is designed imposing performance constraints via H_∞ weighting functions. In [24] a kinematic vehicle model is used and an LPV state feedback steering control has been designed using the polytopic approach, with varying parameters the longitudinal speed and the look-ahead distance. Furthermore, LPV control theory has been used to tackle an online planning application for race autonomous vehicles [25], where LPV was used to reformulate a non-linear vehicle model into a pseudo-linear expressing it in an LPV form and consequently convexify an objective function to be included in a MPC formulation.

The main objective and contribution of this paper are to develop an LPV gain-scheduling (i.e. gridded-based) strategy for the design of a lateral controller for autonomous vehicles able to handle the whole operating domain of longitudinal speed (i.e. speed is treated as varying parameter) as well as the variation of the look-ahead time. Combining a dynamical vehicle model with look-ahead dynamics, together with an identified actuator model including an input delay, the closed-loop performances can be achieved and the tracking capabilities can be improved for every speed. This is obtained in particular through *ad hoc* representation of the look-ahead time as a parameter-dependent function. An H_∞/LPV control problem is formulated considering parameter-dependent weighting functions, allowing the control adaptation for all speeds. The synthesis is performed using the gridding approach, in order to account for varying parameter rate. Therefore stability and performance are maintained along all parameter trajectories. It is worth noting that the development and experimental validation of the proposed gridded-based approach is new in this context. The main contributions are summarized below:

- Using LPV theory combined with look-ahead and actuator dynamics, the lateral control problem can be parameterized by only one parameter i.e. the longitudinal speed.
- The proposed gain-scheduled controller can handle the whole operating domain of longitudinal speeds, using a tunable H_∞ parameter-dependent weighting function.
- That function is the look-ahead time that limits the steering command properly to satisfy the current control objectives, which is of great importance in real cars: the higher the speed, the lower the vehicle turning capabilities.
- The tracking performance can achieve small lateral errors, as its shown experimentally from the testing of the embedded gain-scheduled controller on a Electric Renault Zoe.

This paper is organised as follows. Section 2 describes the modelling of the vehicle combining the look-ahead dynamics and the actuator model. Section 3 introduces briefly the LPV polytopic controller and presents the basics of the LPV gain-scheduled control theory. Then, the LPV model formulation as well as the control objectives are introduced. Moreover, the control synthesis procedure is detailed and the validation of the proposed control in the frequency domain. Section 4 describes the simulation scenario and the associated results for the two LPV controllers. Section 5 shows the experimental results in a test track for a varying speed profile and the analysis of the implementation of the LPV controllers. Section 6 concludes the paper.

II. Lateral Control Framework

The lateral vehicle dynamics can be modeled as a two-wheeled bicycle model [26]. Using this model and by parameterizing the longitudinal speed of the vehicle, the yaw dynamics can be decoupled and a steering controller can be designed regardless of the longitudinal dynamics of the vehicle.

Fig. 1 shows the resulting vehicle model which is expressed by the parameters where v_x and v_y are the longitudinal and lateral velocity accordingly. $\dot{\psi}$ is the yaw rate of the car. α_f, α_r are the tire side-slip angles of the front and rear wheels respectively. β is the side slip angle of the vehicle body. δ is the steering wheel angle. L_f, L_r are the distances of the front and rear wheel from the center of the gravity of the car and C_f, C_r the front and rear cornering stiffness. The lateral tire forces are approximated as linear functions:

$$\begin{aligned} F_{yf} &= C_f \alpha_f \\ F_{yr} &= C_r \alpha_r \end{aligned} \tag{1}$$

Using small angles approximations, the side slip angles can be written as:

$$\begin{aligned} \alpha_f &= \delta - \frac{v_y + L_f \dot{\psi}}{v_x} \\ \alpha_r &= \frac{-v_y + L_r \dot{\psi}}{v_x} \end{aligned} \tag{2}$$

Using Newton's second law and the moment balance at the z axis, the next equations are derived:

$$\begin{aligned} m a_y = m(\dot{v}_y + v_x \dot{\psi}) &= F_{yf} + F_{yr} \\ I_z \ddot{\psi} &= L_f F_{yf} - L_r F_{yr} \end{aligned} \tag{3}$$

where a_y is the lateral acceleration, m the mass and I_z the car inertia.

Considering v_y and $\dot{\psi}$ as state variables and combining the equations (1), (2), (3) the linear vehicle model in state space

form is derived:

$$\begin{bmatrix} \dot{v}_y \\ \ddot{\psi} \end{bmatrix} = \begin{bmatrix} -\frac{C_f + C_r}{m v_x} & -v_x + \frac{C_r L_r - C_f L_f}{m v_x} \\ \frac{-L_f C_f + L_r C_r}{I_z v_x} & -\frac{L_f^2 C_f + L_r^2 C_r}{I_z v_x} \end{bmatrix} \begin{bmatrix} v_y \\ \dot{\psi} \end{bmatrix} + \begin{bmatrix} \frac{C_f}{m} \\ \frac{L_f C_f}{I_z} \end{bmatrix} \delta \tag{4}$$

A. Look-ahead Dynamics

Fig. 2 presents the look-ahead system [27], where y_L is the lateral offset from the reference trajectory at a target point in a distance L away from the vehicle. ε_L is the angular error between the reference heading at the target point and the vehicle's orientation. Considering y_L and ε_L as state variables, the equations that describe their evolution are:

$$\begin{aligned} \dot{y}_L &= -v_y - L\dot{\psi} + v_x \varepsilon_L \\ \dot{\varepsilon}_L &= \dot{\psi}_{ref} - \dot{\psi} \end{aligned} \tag{5}$$

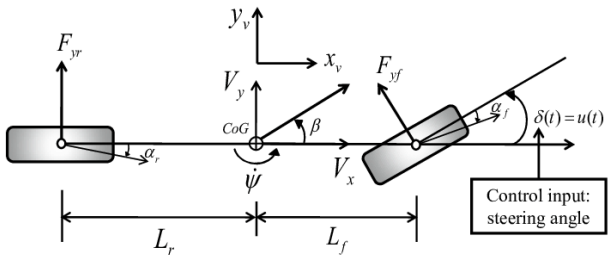

Fig. 1. Two-wheeled bicycle model representing the vehicle lateral dynamics.

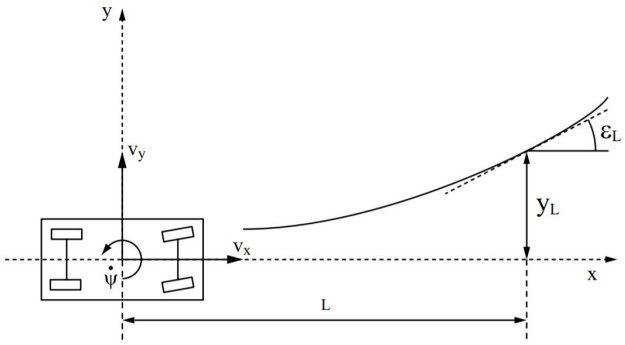

Fig. 2. Look-ahead errors according to the reference trajectory.

B. Combined vehicle model

Combining the state space equations (4), (5), and considering that only the lateral error y_L is measured, the proposed vehicle model is derived as follows:

$$\begin{aligned} \dot{x}_v(t) &= A_v x_v(t) + B_{v_1} w(t) + B_{v_2} u(t) \\ y(t) &= C_v x_v(t) \end{aligned} \tag{6}$$

$$x_v(t) = \begin{bmatrix} v_y \\ \dot{\psi} \\ y_L \\ \varepsilon_L \end{bmatrix}, \; B_{v_1} = \begin{bmatrix} 0 \\ 0 \\ 0 \\ 1 \end{bmatrix}, \; B_{v_2} = \begin{bmatrix} \frac{C_f}{m} \\ \frac{L_f C_f}{I_z} \\ 0 \\ 0 \end{bmatrix},$$

$$A_v = \begin{bmatrix} -\frac{C_f + C_r}{m v_x} & -v_x + \frac{C_r L_r - C_f L_f}{m v_x} & 0 & 0 \\ \frac{-L_f C_f + L_r C_r}{I_z v_x} & -\frac{L_f^2 C_f + L_r^2 C_r}{I_z v_x} & 0 & 0 \\ -1 & -L & 0 & v_x \\ 0 & -1 & 0 & 0 \end{bmatrix},$$

$C = \begin{bmatrix} 0 & 0 & 1 & 0 \end{bmatrix}$.

where $x_v(t)$ is the combined state vector, $w(t) = \dot{\psi}_{ref}$ is the exogenous input, $u(t) = \delta$ the control input and $y(t) = y_L$ is the measurement used for feedback.

C. Extended vehicle-actuator model

Steering actuator dynamic plays a key role when it comes to design a lateral control system. A second order transfer function of the actuator model has been identified in the form below:

$$G_{act} = \frac{k}{s^2 + 2\zeta w_n s + w_n^2} e^{-T_d s}$$

where k, ζ, w_n and T_d are the static gain, the damping, the natural frequency and the time delays respectively. In state space the actuator model can be written as follows:

$$\begin{aligned} \dot{x}_{act}(t) &= A_{act} x_{act}(t) + B_{act} u(t) \\ u_{act}(t) &= C_{act} x_{act}(t) + D_{act} u(t) \end{aligned} \tag{7}$$

For control design purpose, a second order Padé approximation of the time delay has been chosen. Therefore, $x_{act} \in \mathbb{R}^4$ is the vector expressing the states of the actuator, $A_{act} \in \mathbb{R}^{4\times4}$, $B_{act} \in \mathbb{R}^{4\times1}$, $C_{act} \in \mathbb{R}^{1\times4}$, $D_{act} \in \mathbb{R}^{1\times4}$ are the systems matrices and $u_{act} \in \mathbb{R}$ is the output.

Considering the output of the actuator as the input of the vehicle model leads to the extended equation:

$$\dot{x}_v(t) = A_v x_v(t) + B_{v_1} w(t) + B_{v_2} [C_{act} x_{act}(t) + D_{act} u(t)]$$

Consequently, the extended model can be given as:

$$\begin{aligned} \dot{x} &= Ax(t) + B_1 w(t) + B_2 u(t) \\ y &= Cx \end{aligned} \tag{8}$$

where $x(t) = \left[\frac{x_v(t)}{x_{act}(t)}\right] \in \mathbb{R}^8$ is the extended state vector, $A = \left[\begin{array}{c|c} A_v & B_{v_2}C_{act} \\ \hline 0 & A_{act} \end{array}\right] \in \mathbb{R}^{8\times 8}$, $B_1 = \left[\frac{B_{v_1}}{0}\right] \in \mathbb{R}^8$, $B_2 = \left[\frac{B_{v_2}D_{act}}{B_{act}}\right] \in \mathbb{R}^8$ and $C = [C_v \ 0] \in \mathbb{R}^{1\times 8}$ are the extended system matrices.

III. LPV Controller Design

This section presents the LPV methodology developed in this study to design a dynamic output controller. Let us recall that three approaches are mostly used for the representation of an LPV model and then for LPV control synthesis: 1) Polytopic Set of Parameters; 2) Linear Fractional Transformation; and 3) Set of Gridded Parameter Points. The last one is proposed in this paper using a gain-scheduling approach for the lateral vehicle control system. For comparison purposes, a more classical approach based on a LPV polytopic controller is also carried out. Benefits of the gridded-based approach are theoretically and experimentally demonstrated with respect to polytopic one.

This section firstly introduces the polytopic controller design. Then, the basics of the LPV gain-scheduled controller are presented. The LPV model formulation and the considered control objectives are presented afterwards. Finally, the LPV control scheme, the problem solution as well as the analysis of the solution in the frequency domain are presented.

A. LPV Polytopic Controller

For comparison purposes, a LPV controller based on the polytopic approach [28] is designed. The referred-to-as polytopic method is restricted to LPV systems whose matrices are depending in an affine way on the vector of parameters. Moreover the parameters are assumed to be known and bounded i.e.:

$$\underline{\rho_j} \leq \rho_j \leq \overline{\rho_j}$$

where ρ_j is the j^{th} element of the varying parameter vector , and $\overline{\rho_j}$, $\underline{\rho_j}$ are the upper and lower bounds respectively. The set of varying parameters is then a polytope with 2^n vertices, where n is the number of the varying parameters, and the system matrices can be written as

$$\left[\begin{array}{c|c} A(\rho) & B(\rho) \\ \hline C(\rho) & D(\rho) \end{array}\right] = \sum_{i=1}^{2^n} a_i \left[\begin{array}{c|c} A_i & B_i \\ \hline C_i & D_i \end{array}\right] \tag{9}$$

In the LPV/H_∞ framework, the control synthesis problem is treated off-line by solving a set of LMIs at each vertex of the polytope using convex optimization. The solution of the problem are the state space representations of the vertex LTI controllers, K_i, where $1 \leq i \leq 2^n$.

The polytopic LPV controller $K(\rho)$ is computed on-line as the convex combination of the vertex controllers K_i.

$$\begin{aligned} K(\rho) &= \sum_{i=1}^{2^n} a_i(\rho) K_i \\ a_i(\rho) &= \frac{\prod_{j=1}^{n} |\rho_j - C^c(\omega_i)_j|}{\prod_{j=1}^{n} (\overline{\rho_j} - \underline{\rho_j})} > 0 \\ \sum_{i=1}^{2^n} a_i(\rho) &= 1 \end{aligned} \tag{10}$$

where $C^c(\omega_i)_j$ is the j^{th} element of the vector $C^c(\omega_i)$, as follows:

$$C^c(\omega_i)_j = \begin{cases} \overline{\rho_j} & if \ \omega_i = \underline{\rho_j} \\ \underline{\rho_j} & otherwise \end{cases}$$

B. Background on the LPV Gridding Approach

Before introducing the LPV modelling of the state space equations of the system, let us recall the basics of the LPV Gain scheduled Gridded Controller for a simplified case in order to present the explicit solution. The interested reader may find more details in [29], [30].

Definition 1. Generalized LPV System
A dynamical LPV system can be expressed by the following state space equations:

$$\Sigma(\rho): \begin{bmatrix} \dot{x}(t) \\ \hline z(t) \\ y(t) \end{bmatrix} = \left[\begin{array}{c|cc} A(\rho) & B_1(\rho) & B_2(\rho) \\ \hline C_1(\rho) & D_{11}(\rho) & D_{12}(\rho) \\ C_2(\rho) & D_{21}(\rho) & D_{22}(\rho) \end{array}\right] \begin{bmatrix} x(t) \\ \hline w(t) \\ u(t) \end{bmatrix} \tag{11}$$

where $x(t) \in \mathbb{R}^n$ express the states of the system, $w(t) \in \mathbb{R}^{n_w}$ are the exogenous inputs, $u(t) \in \mathbb{R}^{n_w}$ the control input, $z(t) \in \mathbb{R}^{n_z}$ controlled outputs, $y(t) \in \mathbb{R}^{n_y}$ hold for the system's measurements. $A(\rho) \in \mathbb{R}^{n\times n}$, $B_1(\rho) \in \mathbb{R}^{n\times n_w}$, $B_2(\rho) \in \mathbb{R}^{n\times n_u}$, $C_1(\rho) \in \mathbb{R}^{n_z\times n}$, $C_2(\rho) \in \mathbb{R}^{n_y\times n}$, $D_{11}(\rho) \in \mathbb{R}^{n_z\times n_w}$, $D_{12}(\rho) \in \mathbb{R}^{n_z\times n_u}$, $D_{21}(\rho) \in \mathbb{R}^{n_y\times n_w}$ and $D_{22}(\rho) \in \mathbb{R}^{n_y\times n_u}$. $\rho = [\rho_1(t) \ \rho_2(t) \ .. \ \rho_s(t)] \in \Omega$ (convex set) and $|\dot{\rho}(t)| \leq v_i$ $(i = 1,2,..,s)$ is a vector of time varying parameters, assumed to be known and bounded $\forall t$.

For the purpose of simplification, the following assumptions (Δ_{1-4}) are made on the LPV Generalized state space system.

$\Delta_1 : D_{11}(\rho) = 0_{n_z\times n_w}$
$\Delta_2 : D_{22}(\rho) = 0_{n_y\times n_u}$
$\Delta_3 : D_{12}(\rho)$ is of full column rank for all $\rho \in \Omega$
$\Delta_4 : D_{21}(\rho)$ is of full row rank for all $\rho \in \Omega$

Definition 2. Simplified Generalized LPV System
Taking into account the previous assumptions, a dynamical LPV system can be expressed by the following state space

equations:

$$S(\rho): \begin{bmatrix} \dot{x}(t) \\ \hline z_1(t) \\ z_2(t) \\ y(t) \end{bmatrix} = \left[\begin{array}{c|ccc} A(\rho) & B_{11}(\rho) & B_{12}(\rho) & B_2(\rho) \\ \hline C_{11}(\rho) & 0 & 0 & 0 \\ C_{12}(\rho) & 0 & 0 & I_{n_{w_2}} \\ C_2(\rho) & 0 & I_{n_{z_2}} & 0 \end{array}\right] \begin{bmatrix} x(t) \\ \hline w_1(t) \\ w_2(t) \\ u(t) \end{bmatrix} \tag{12}$$

where $B_1(\rho) = [B_{11}(\rho) \;\; B_{12}(\rho)]$, $C_1(\rho) = [C_{11}(\rho) \;\; C_{12}(\rho)]$.

Definition 3. LPV Controller
An LPV Controller can be described in the following form:

$$K(\rho): \begin{bmatrix} \dot{x}_c(t) \\ u(t) \end{bmatrix} = \begin{bmatrix} A_c(\rho) & B_c(\rho) \\ C_c(\rho) & D_c(\rho) \end{bmatrix} \begin{bmatrix} x_c(t) \\ y(t) \end{bmatrix} \tag{13}$$

where $x_c(t) \in \mathbb{R}^{n_c}$ define the states of the LPV controller. $A_c(\rho) \in \mathbb{R}^{n_c \times n_c}$, $B_c(\rho) \in \mathbb{R}^{n_c \times n_y}$, $C_c(\rho) \in \mathbb{R}^{n_u \times n_c}$ and $D_c(\rho) \in \mathbb{R}^{n_u \times n_y}$.

The control objective considered for the closed-loop LPV system is to minimize the L_2-norm from the disturbance to error signal, i.e. to provide disturbance/error attenuation. Let us recall that the induced L_2-norm of an LPV system [31] is defined as:

$$\|G\| = \sup_{\rho \in \Omega} \sup_{\|w\| \neq 0} \frac{\|z\|_2}{\|w\|_2} \tag{14}$$

Below, is presented the theorem from [30] as the solution of the control synthesis problem for the minimization of (14). Given a compact set $\Omega \subset \mathbb{R}^s$, non-negative $\{v_i\}_{i=1}^s$ numbers, performance level $\gamma > 0$, and the open-loop LPV system in (12), the LPV synthesis γ-performance/ v-variation problem is solvable if and only if there exist continuously differentiable matrix functions $X : \mathbb{R}^s \to \mathbb{R}^{n \times n}$ and $Y : \mathbb{R}^s \to \mathbb{R}^{n \times n}$, such that for all $\rho \in \Omega$, $X(\rho) \succ 0$, $Y(\rho) \succ 0$ and the set of Linear Matrix Inequalities (LMIs) expressed by (15) is satisfied. where:

$$\hat{A}(\rho) = A(\rho) - B_2(\rho)C_{12}(\rho),$$
$$\tilde{A}(\rho) = A(\rho) - B_{12}(\rho)C_2(\rho).$$

Using this control synthesis procedure, the existence of such a parameter-dependent controller $K(\rho)$ is determined. That controller will stabilize the closed-loop LPV system and guarantee the induced L_2-norm performance of the closed-loop system less or equal than $\gamma > 0$.

Solving the set of LMIs (15), an n-dimensional strictly proper controller (13) is defined in state space form, which aims at minimizing (14), where:

$$A_c(\rho) = \big[A(\rho) + \gamma^{-1}[Q^{-1}(\rho)X(\rho)L(\rho)B_{12}^T$$
$$+ B_1(\rho)B_1^T(\rho)]Y^{-1}(\rho) + B_2(\rho)F(\rho) +$$
$$Q^{-1}(\rho)X(\rho)L(\rho)C_2(\rho) - Q^{-1}(\rho)H(\rho,\dot{\rho})\big],$$
$$B_c(\rho) = -\big[Q^{-1}(\rho)X(\rho)L(\rho)\big],$$
$$C_c(\rho) = F(\rho),$$

with

$$Q(\rho) = \big[X(\rho) - Y(\rho)^{-1}\big],$$
$$F(\rho) = -\big[\gamma B_2^T(\rho)Y^{-1}(\rho) + C_{12}(\rho)\big],$$
$$L(\rho) = -\big[\gamma X^{-1}C_2^T(\rho) + B_{12}(\rho)\big],$$
$$H(\rho,\dot{\rho}) = -\Bigg[A_F^T(\rho)Y^{-1} + Y^{-1}A_F(\rho) + \sum_i \left(\dot{\rho}\frac{\partial Y^{-1}}{\partial \rho}\right) +$$
$$\gamma^{-1}C_F^T(\rho)C_F(\rho) + \gamma^{-1}Y^{-1}(\rho)B_1(\rho)B_1^T(\rho)Y^{-1}(\rho)\big]$$

In this way, the LPV control problem is tackled directly avoiding the need of design a LTI controller for each value of the parameter.

Scalar differentiable basis functions has to be chosen $\{f_i : \mathbb{R}^s \to \mathbb{R}\}_{i=1}^N$ and $\{g_i : \mathbb{R}^s \to \mathbb{R}\}_{i=1}^N$ to express $X(\rho)$, $Y(\rho)$ accordingly and optimize (15) over $\{X_i\}_{i=1}^N$, $X_i \in \mathbb{R}^{n \times n}$ and $\{Y_i\}_{i=1}^N$, $Y_i \in \mathbb{R}^{n \times n}$.

$$X(\rho) = \sum_{i=1}^N f_i(\rho)X_i$$
$$Y(\rho) = \sum_{i=1}^N g_i(\rho)Y_i$$

As a last step, selecting a grid of the parameter space Ω by M points $\{\rho_k\}_{k=1}^M$, a finite dimensional convex optimization problem is obtained.

Finally, a grid of LTI state-space controllers is obtained where a linear interpolation between the grid points is performed for the implementation of the LPV gain-scheduled controller.

C. LPV Model Formulation

The state space representation described in (8) can be rewritten as a dynamical LPV system. Defining the look-ahead time as a function of speed $T(v_x)$, the only parameter remaining is the longitudinal speed i.e $\rho = v_x$.

An intensive simulation study for fixed speeds has been carried out and the selected values of the look-ahead time per speed are the ones that satisfy the control objectives described in section 3.4. Performing an interpolation to fit the data, has allowed to model the look-ahead time in the following exponential form:

$$T(v_x) = a\mathrm{e}^{bv_x} + c\mathrm{e}^{dv_x} \tag{16}$$

where $a = 3.83$, $b = -0.7261$, $c = 1.154$ and $d = -0.01453$. Figure 3 depicts the look-ahead time in function of the vehicle speed.

From (8) it can be seen now that the only matrix or vector that contains the v_x is the matrix A. Thus, the LPV model having as states the vehicle model and the states of the actuator model is written as:

$$\begin{aligned} \dot{x} &= A(\rho)x(t) + B_1 w(t) + B_2 u(t) \\ y(t) &= Cx(t) \end{aligned} \tag{17}$$

$$
\begin{bmatrix}
Y(\rho)\hat{A}^T(\rho)+\hat{A}(\rho)Y(\rho)-\sum_{i=1}^{s}\pm\left(v_i\frac{\partial Y(\rho)}{\partial \rho_i}\right)-\gamma B_2(\rho)B_2^T(\rho) & Y(\rho)C_{11}^T(\rho) & B_1(\rho) \\
C_{11}(\rho)Y(\rho) & -\gamma I_{n_{z_1}} & 0 \\
B_1^T(\rho) & 0 & -\gamma I_{n_w}
\end{bmatrix} \prec 0
$$

$$
\begin{bmatrix}
\tilde{A}^T(\rho)X(\rho)+X(\rho)\tilde{A}(\rho)+\sum_{i=1}^{s}\pm\left(v_i\frac{\partial X(\rho)}{\partial \rho_i}\right)-\gamma C_2^T(\rho)C_2(\rho) & X(\rho)B_{11}^T & C_1(\rho) \\
B_{11}^T(\rho)X(\rho) & -\gamma I_{n_{w_1}} & 0 \\
C_1^T(\rho) & 0 & -\gamma I_{n_z}
\end{bmatrix} \prec 0 \tag{15}
$$

$$
\begin{bmatrix} X(\rho) & I_n \\ I_n & Y(\rho) \end{bmatrix} \succeq 0
$$

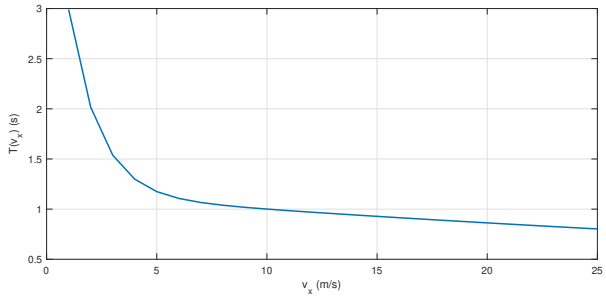

Fig. 3. Look-ahead time in function of the speed

where $x(t)=\begin{bmatrix} x_v(t) \\ \hline x_{act}(t) \end{bmatrix} \in \mathbb{R}^8$ is the extended state vector,and $A(\rho)=\left[\begin{array}{c|c} A_v(\rho) & B_{v_2}C_{act} \\ \hline 0 & A_{act} \end{array}\right]$, with

$$
A_v(\rho)=\begin{bmatrix}
-\frac{C_f+C_r}{m\rho} & -\rho+\frac{C_rL_r-C_fL_f}{m\rho} & 0 & 0 \\
\frac{-L_fC_f+L_rC_r}{I_z\rho} & -\frac{L_f^2C_f+L_r^2C_r}{I_z\rho} & 0 & 0 \\
-1 & -\rho T(\rho) & 0 & \rho \\
0 & -1 & 0 & 0
\end{bmatrix},
$$

$$
C=\begin{bmatrix} 0 & 0 & 1 & 0 & 0 & 0 & 0 & 0 \end{bmatrix}
$$

The other matrices remain unchanged. As it was previously stated, lateral error y_L is the only measurement used in the feedback control.

D. Control Objectives

According to the Pure-Pursuit algorithm [32], the control of the vehicle is achieved by minimizing the lateral error at the target point. At the same time, look-ahead time is a design parameter since target points depends on it—i.e the look-ahead distance is affected ($L=v_xT$). For small look-ahead distance, the target points are located close to the vehicle and since the main goal is to reach these points, the vehicle will react quickly. On the contrary, when the target points are chosen to be far from the vehicle's position, then the vehicle will respond slower. Hence, it is clear that the look-ahead time is a parameter that affects the bandwidth of the closed-loop system.

Here lies the question of how far or how close should the target point be in order for the vehicle to follow the desired trajectory and simultaneously keep comfort. This paper combines the look-ahead time with the weight on the lateral error at the target point for low and high speeds to achieve good performance.

The control objectives conceived to perform optimal lane-tracking are as follows:

- For low speeds ($u_x < 10\ m/s$), fast turning capabilities are required. For that reason, the look-ahead distance is chosen to be small and the weight on the lateral error at the target point to be big.
- For higher speeds ($u_x > 10\ m/s$), the vehicle has not to steer much in order to reach the control point. Thus, the look-ahead distance is chosen to be higher and the weight on the lateral error decreases for higher speeds.
- The steering wheel angle should track the desired trajectory but also sustain comfort as well i.e the bandwidth of the controller should be less than 1 rad/s.
- The look-ahead time has to be the minimum one for lane tracking without causing overshoots and oscillations of the vehicle response.

E. Control Structure & Synthesis

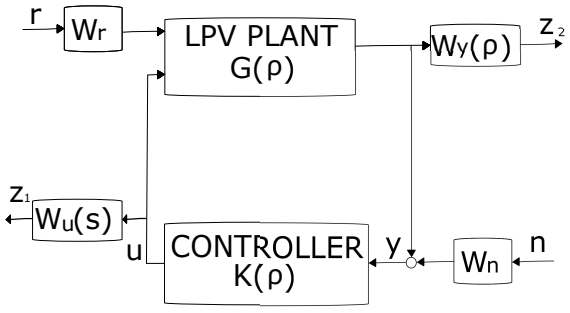

Fig. 4. LPV Control Scheme

Fig. 4 presents how the proposed methodology is formulated in the LPV framework. In this control scheme is included the LPV plant (17), the grid-based controller, the performance output vector z and the weighting functions W_r,

W_n, $W_u(s)$ and $W_y(\rho)$. The signals $n(t)$ and $r(t)$ represent noise signal imposed additively on the measurement y_L and the weighted reference $\dot{\psi}_{ref}$ respectively.

The weighting function $W_y(\rho)$ is chosen as $W_y(\rho) = T(\rho)$. In this way, the proposed methodology is applied by imposing higher weights for low speeds on the lateral error at the target point.

The filter $W_u(s)$ is chosen as $W_u(s) = \dfrac{s + \frac{w_{bc}}{M}}{\varepsilon s + w_{bc}}$ with $w_{bc} = 0.5$ rad/s to respect the corresponding control objective about the bandwidth of the controller ($w_{bc} < 1$ rad/s), $M = 2$ ($6db$) to respect the saturation limits and $\varepsilon = 0.1$ (10^{-1} rad/s) that expresses the frequency where the roll-off starts to achieve better noise attenuation.

Finally, constant weights are added as: $W_n = 0.5$ and $W_r = 0.1$.

Extending the system (17) with the the weighting functions, exogenous inputs and controlled outputs, leads to the generalized plant of the system.

$$\begin{bmatrix} \dot{x}(t) \\ z(t) \\ y(t) \end{bmatrix} = \left[\begin{array}{c|cc} A(\rho) & B_1 & B_2 \\ \hline C_1(\rho) & D_{11} & D_{12} \\ C_2 & D_{21} & 0 \end{array}\right] \begin{bmatrix} x(t) \\ w(t) \\ u(t) \end{bmatrix} \tag{18}$$

where x is the extended state vector combining the vehicle, actuator and weighting functions state variables, $w(t) = [r(t)\ n(t)]^T$ are the new vector with the exogenous inputs and $z = [z_1\ z_2]^T$ the controlled outputs.

F. Problem Solution & Analysis in the Frequency Domain

Fig. 4 presents the interconnections for the LPV control synthesis. The problem solution has been computed using *LPVTools* toolbox [33]. The generalized plant (18) is gridded for frozen values of the parameter $\rho = 5:1:25$ m/s and as parameter variation bounds are imposed $-9 \leq \dot{\rho} \leq 3$ taking into consideration braking and accelerating bounds. The basis functions f_i and g_i to construct $X(\rho)$ and $Y(\rho)$ are picked as second order polynomial functions judging by simulations, since no concrete methodology exists about their selection.

$$X(\rho) = X_0 + \rho X_1 + \rho^2 X_2$$

$$Y(\rho) = Y_0 + \rho Y_1 + \rho^2 Y_2$$

Finally, the set of LMIs (15) formed at the grid points of the generalized plant (18) are solved for γ and X_i and Y_i. At that point, with $\gamma = 0.9752$, the reconstruction of LTI state space controllers takes place for each grid point of the speed.

Figure 5 presents the frequency response for all speeds from steering wheel angle to the reference yaw rate relatively to the specification imposed by the template weighting function W_u. Fig 6 shows the bode plot for all speeds from the lateral error at the target point to the reference yaw rate for the closed-loop system. It has to be remarked that since $\gamma < 1$, the control objectives are met. Fig. 7 shows the frequency response of the LTI controllers corresponding for all gridded points of speed. As speed increases, the output of the controller decreases as is demanded in the control objectives.

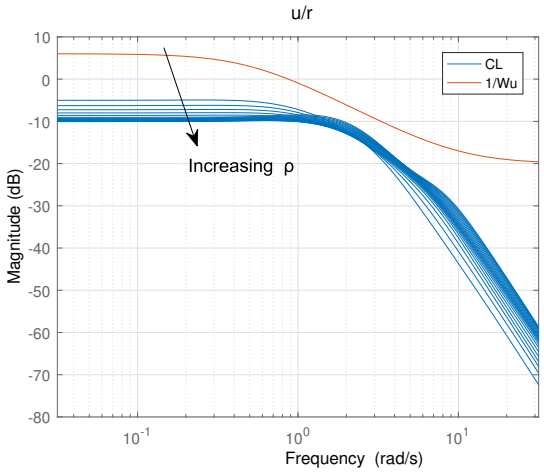

Fig. 5. Controller Sensitivity of the closed-loop system. The arrow shows the direction of the increasing parameter ρ.

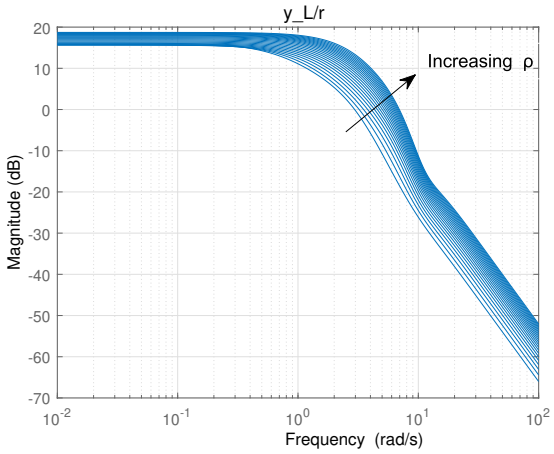

Fig. 6. Frequency response $\frac{y_L}{r}$ of the closed-loop system. The arrow shows the direction of the increasing parameter ρ.

IV. Performance Assessment using Time-Domain Simulations

A. About the design of the polytopic controller

The LPV controller based on the polytopic approach is designed for comparison based on the vehicle model presented in (6) without the actuator model. This choice is taken in order to avoid higher order controller and implementation issues that may occur.

It is worth noting that the LPV matrices in (6) can not be written in an affine form from the only parameter $\rho = v_x$, since the term $\frac{1}{v_x}$ is also included in the A_v matrix. Therefore, to apply the polytopic aprroach, we must consider two parameters, $\rho_1 = v_x$ and $\rho_2 = \frac{1}{v_x}$. Thus, the vertices ω_i of the polytope will be $2^2 = 4$ defined by the combinations of the upper and lower bounds of these two parameters, where $v_x \in [5, 25]$.

To avoid further enlargement of the polytope, the look-ahead time is here selected constant $T = 1.2s$, which is a

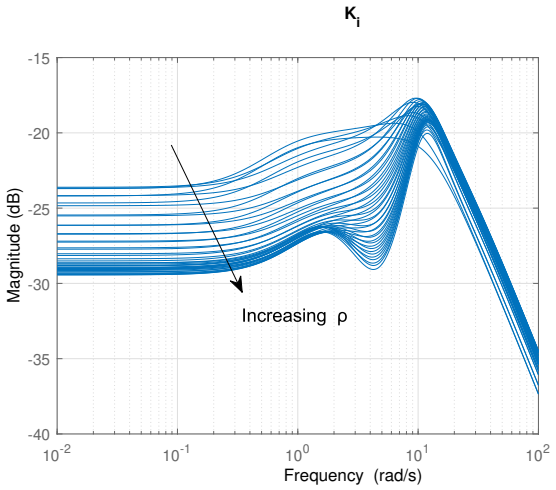

Fig. 7. Frequency response of the LTI gain-scheduled controller K_i. The arrow shows the direction of the increasing parameter ρ.

limitation. Note that, in the case where the look-ahead time is treated as a parameter, a structure with three parameters must be considered which leads to very conservative results.

Solving a set of LMIs at each vertex of the polytope via Yalmip [34], the solution of the problem occurred which are the vertex LTI controllers, $K_i = \begin{bmatrix} A_i & B_i \\ C_i & D_i \end{bmatrix}$, where $1 \leq i \leq 4$ and on-line the polytopic LPV controller is calculated according to (10).

B. Comparison of the Results

A simulation scenario that combines an initial lateral error with a sharp turn is designed to evaluate controller capabilities to handle initial errors and tracking capabilities in turns. Figure 8 plots the reference trajectory. The vehicle starts with an initial error of a meter away from the reference, then it follows a straight line and finally, it should track a turn with a radius $R = 100m$.

First, Fig. 9 shows the lateral error at center of gravity of the vehicle for the two LPV controllers for speed $v_x = 5m/s$ where the look-ahead time is $T = 1.2s$ for both controllers. Fig. 10, 11, 12, 13 show the lateral error at center of gravity of the vehicle for the two LPV controllers for speeds $v_x = 10, 15, 20, 25m/s$ respectively where $T = 1.2s$ remains constant for the polytopic and for the gain-scheduled changes according to (16).

For speeds $v_x \leq 10m/s$ in Fig. 9, 10, starting from one meter away, the polytopic controller reaches the desired lane without overshoots. As speed increases, oscillations start to appear as a sign of losing performance for the polytopic controller. On the contrary, the gain-scheduled controller is capable of handling even such an initial error and only for $v_x = 25m/s$ small oscillations appear in Fig. 13.

At the part of the turn, the polytopic controller provides good performance (i.e. small lateral errors less than $0.5m$) again for $v_x = 5, 10m/s$ (see Fig. 9, 10). It has to be remarked that even when the look-ahead time $T = 1.2s$ is the same for both controllers in Fig. 9, the gain-scheduled achieves smaller lateral error than the polytopic one. As the speed increases in the case of the polytopic controller, the lateral error continues to increase in the turn reaching even $1.5m$ for $v_x = 25m/s$ in Fig. 13. Instead, in the case of the gridded controller, it can be seen that for speeds $v_x \leq 15m/s$, the lateral error never exceeds $0.2m$ (see Fig. 9, 10, 11), and for $v_x = 20, 25m/s$ never gets more than $0.4m$ (see Fig. 12, 13).

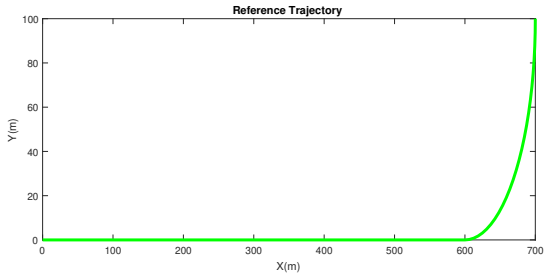

Fig. 8. Reference trajectory used for simulation. (Simulations)

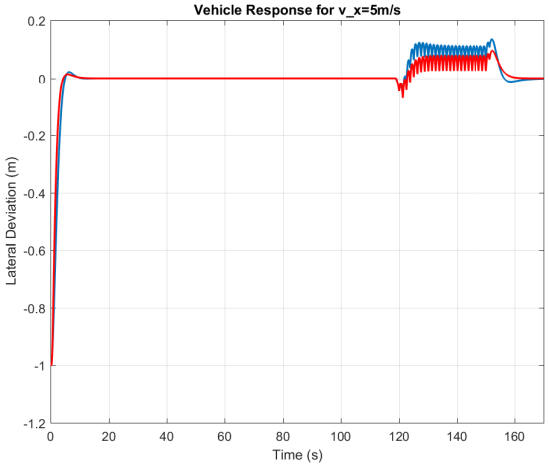

Fig. 9. Lateral deviation response for speed test $v_x = 5m/s$ and look-ahead time $T = 1.2s$ for both of the LPV controllers. Polytopic is in blue and gain-scheduled in red. (Simulations)

V. Experimental Results

The proposed lateral controller has been implemented on an automated Renault ZOE (see Fig. 14). Experiments were carried out in a private test track located in Satory, 20 km away of Paris, France. The vehicle is equipped with a Real-Time Kinematic Differential Global Positioning System (RTK-DGPS) that serves as precise positioning system. A MicroAutoBox is installed in the trunk. It receives both the vehicle positioning and reference trajectory via Ethernet connection from an industrial computer.

A. Implementation Issues

The implementation of the polytopic and gridded LPV controllers on the experimental platform is a two-step procedure:

1) The LTI controllers (for every vertex for the polytopic case and for every selected frozen value of the speed

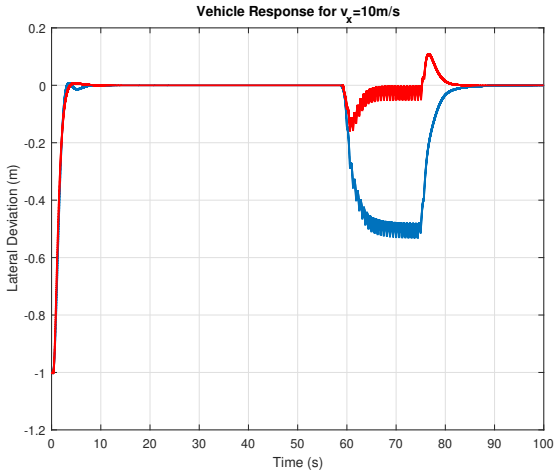

Fig. 10. Lateral deviation response for speed test $v_x = 10m/s$ and $T = 1.2s$ for the polytopic, for the gain-scheduled from eq. (16). Polytopic is in blue and gain-scheduled in red. (Simulations)

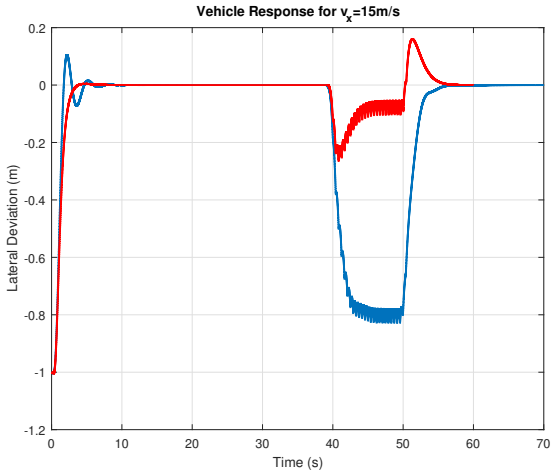

Fig. 11. Lateral deviation response for speed test $v_x = 15m/s$ and $T = 1.2s$ for the polytopic, for the gain-scheduled from eq. (16). Polytopic is in blue and gain-scheduled in red. (Simulations)

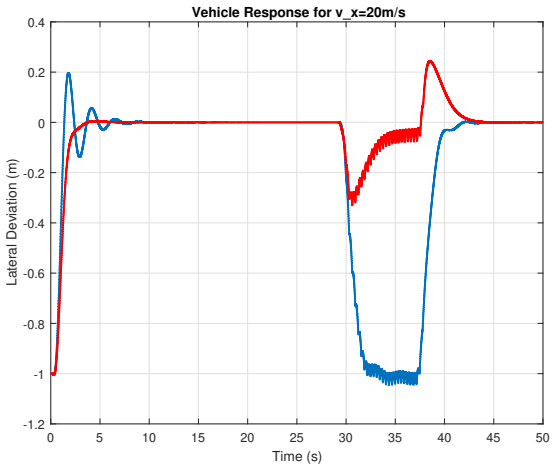

Fig. 12. Lateral deviation response for speed test $v_x = 20m/s$ and $T = 1.2s$ for the polytopic, for the gain-scheduled from eq. (16). Polytopic is in blue and gain-scheduled is in red. (Simulations)

Fig. 13. Lateral deviation response for speed test $v_x = 25m/s$ and $T = 1.2s$ for the polytopic, for the gain-scheduled from eq. (16). Polytopic is in blue and gain-scheduled in red. (Simulations)

for the gridding one) have been discretized for a sampling period $T_s = 0.01s$,

2) At each sample time the controller $K(\rho)$ is realized as a linear interpolation of the two discretized LTI controllers K_{i-1}, K_i for values of the gridded points of the parameters ρ_{i-1}, ρ_i respectively, for which $\rho \in [\rho_{i-1}, \rho_i]$.

$$K(\rho) = a(\rho)K_i + (1 - a(\rho))K_{i-1}$$
$$a(\rho) = \frac{\rho - \rho_{i-1}}{\rho_i - \rho_{i-1}} \tag{19}$$

where $a(\rho)$ is a scaling factor computed on-line for the measured parameter ρ whose value is between ρ_{i-1} and ρ_i.

It is worth noting that, to reduce the complexity of the implementation, it was chosen a smaller number of controllers to be interpolated according to (19) to treat the whole range of speed. More specifically, the controllers chosen were for frozen values of $v_x = 5, 10, 15, 20, 25m/s$, i.e K_i with $i = 1, .., 5$.

Remark: the implementation for the polytopic controller on-line is a convex combination (10) of the discretized vertex LTI controllers. It is worth saying that the discretization of the polytopic controller, since it was carried out for each vertex of the polytope, cannot guarantee the performance/stability that were ensured during the synthesis of the continuous time control. However, this was checked a posteriori before the implementation.

B. Experimental results

Both LPV controllers were implemented on the real vehicle for comparison purposes. Speed profile is provided by the navigation system and, if no interaction with other traffic agents occurs as in this case (tests are done in a

Fig. 14. Automated Electric Renault Zoe

private test track), is identical for both controllers. It is adapted accordingly to the road curvature, assuring comfort on-board. Fig. 15 presents the speed profile during the tests. The autonomous mode is activated when the speed is about $4m/s$. Then, the vehicle accelerates until $14m/s$ in a straight stretch, maintaining the same speed up to second 40 where smoothly decelerates up to $9m/s$. Figure 16 shows the experimental area, which combines a straight stretch with two turns with variable radius, and the trajectories of the two LPV controllers measured during the test.

To assess the lane-tracking capabilities of the two designed LPV controllers, the lateral offset at the vehicle's center of gravity is examined in Fig. 17 and the steering wheel angle in degrees computed from each controller in Fig. 18.

At the beginning of the test where the vehicle accelerates, oscillations are observed under the polytopic control. This can be explained from Fig. 18, where the vehicle turns even 100 degrees. Instead the gridded controller handles this continuous change of speed smoothly without having an increase of lateral error neither by turning jerkily. The steering wheel angle is not changing abruptly keeping comfort at all times. On the other hand, the polytopic controller cannot handle the turns: the lateral error increases more than $1m$ and the controller's output presents oscillations when the speed changes quickly.

Experimental results validate the interest and efficiency of the proposed LPV gain-scheduling control approach for lateral control of autonomous cars.

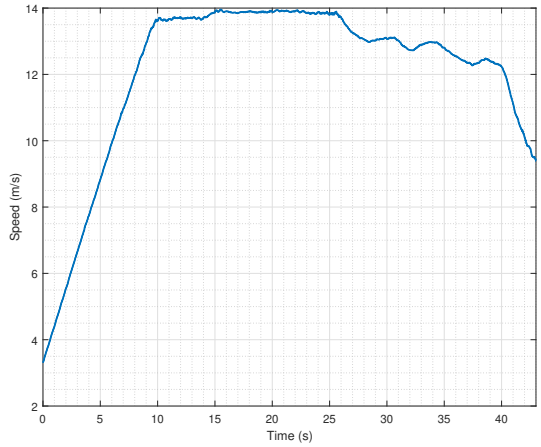

Fig. 15. Longitudinal speed profile during test. (Experiments)

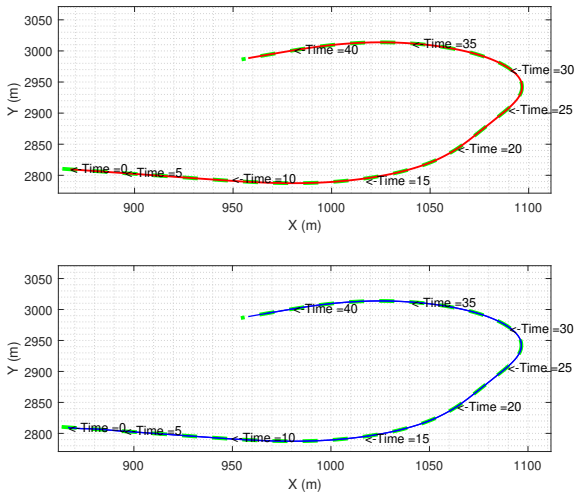

Fig. 16. Figure (top): trajectory followed from the gain-scheduled controller. Figure (bottom): trajectory followed from the polytopic controller. Test track is in green, polytopic in blue and gain-scheduled in red. (Experiments)

VI. Conclusions & Future Works

This paper presents the design, implementation and testing of a novel LPV gain-scheduled controller combined with the Pure-Pursuit algorithm for the lateral control of an autonomous vehicle.

Simulation and experimental results in comparison with a polytopic LPV controller, shown that the LPV gain-scheduled controller has the advantage of including the a priori knowledge of the rate bounds in the design and as a result, there is no deterioration of the performance for quick changes of the parameter, whereas the polytopic introduced oscillations and huge lateral errors. Moreover, its flexible design allows to choose the appropriate look-ahead time for different values of speed to fulfill the control objectives for low and high speeds. In addition, the LPV gain-scheduled controller makes feasible to choose which LTI state space controllers captures the best the vehicle dynamics for the implementation, avoiding in that way the switching between multiple controllers and simultaneously sustaining the desired performance for the vehicle via merely a linear interpolation.

Future works may include the investigation of the robustness of the proposed controller by considering disturbances on the frequency domain, and uncertainties on the vehicle model parameters. Another future step is the design of a prediction-based control scheme to alter the longitudinal speed of the vehicle, taking into account its braking/acceleration capabilities, for overtaking and high-speed maneuvers.

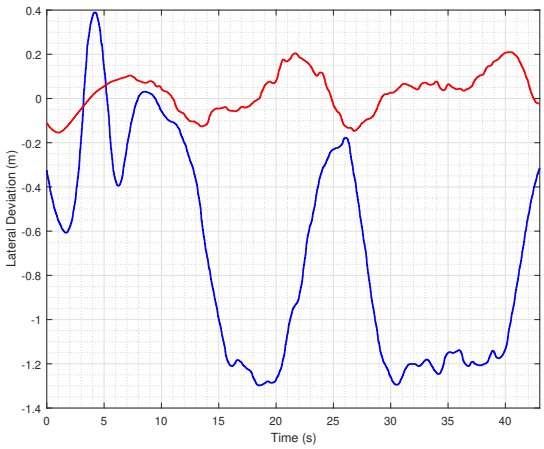

Fig. 17. Lateral deviation response of the vehicle throughout the test. Polytopic is in blue and gain-scheduled in red. (Experiments)

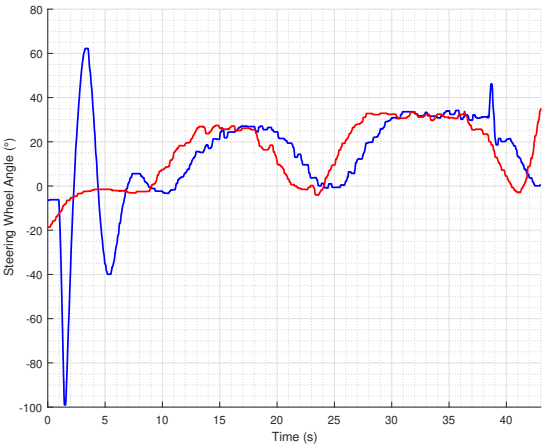

Fig. 18. Steering wheel angle response of the vehicle throughout the test. Polytopic is in blue and gain-scheduled in red. (Experiments)

ACKNOWLEDGMENT

This paper reflects solely the views of the authors and not necessarily the view of the company they belong to.

Authors want to thank David Gonzalez for his support on the controllers integration on the experimental platform and Professor Peter Seiler Jr. for the fruitful discussion on the LPV gain-scheduled controller implementation.

REFERENCES

[1] Gruel, W., Stanford, J. M.: 'Assessing the long-term effects of autonomous vehicles: a speculative approach', *Transp. Res. Proc.*, 2016, **13**, pp. 18–29

[2] González, D., Pérez, J., Milanés, V., Nashashibi, F.: 'A review of motion planning techniques for automated vehicles', *IEEE Trans. Intell. Transp. Syst.*, 2015, **17**, (4), pp. 1135–1145

[3] Shladover, S. E.: 'Review of the state of development of advanced vehicle control systems (AVCS)', *Veh. Syst. Dyn.*, 1995, **24**, (6-7), pp. 551–595

[4] Guo, H., Liu, F., Xu, F., Chen, H., Cao, D., Ji, Y.: 'Nonlinear model predictive lateral stability control of active chassis for intelligent vehicles and its FPGA implementation', *IEEE Trans. Syst. Man Cybern. Syst.*, 2017, **49**, (1), pp. 2–13

[5] Doumiati, M., Sename, O., Dugard, L., Martinez-Molina, J. J., Gaspar, P., Szabo, Z.: 'Integrated vehicle dynamics control via coordination of active front steering and rear braking', *Eur. J. Control*, 2013, **19**, (2), pp. 121–143

[6] Ackermann, J., T. Bünte, D. Odenthal.: 'Advantages of active steering for vehicle dynamics control', (1999)

[7] Jochem, T., Pomerleau, D.: 'Life in the fast lane: The evolution of an adaptive vehicle control system', *AI Mag.*, 1996, **17**, (2), pp. 11–50

[8] Broggi, A., Bertozzi, M., Fascioli, A., Bianco, C. G. L., Piazzi, A.: 'The ARGO autonomous vehicle's vision and control systems', *Int. J. Intell. Control Syst.*, 1999, **3**, (4), pp. 409–441

[9] Thrun, S., Montemerlo, M., Dahlkamp, H., *et al.*: 'Stanley: The robot that won the DARPA Grand Challenge', *J. Field Robot.*, 2006, **23**, (9), pp. 661–692

[10] Xu, P., Dherbomez, G., Héry, E., Abidli, A., Bonnifait, P.: 'System architecture of a driverless electric car in the grand cooperative driving challenge', *IEEE Intell. Transp. Syst. Mag.*, 2018, **10**, (1), pp. 47–59

[11] Falcone, P., Borrelli, F., Asgari, J., Tseng, H. E., Hrovat, D.: 'Predictive active steering control for autonomous vehicle systems', *IEEE Trans. Control Syst. Technol.*, 2007, **15**, (3), pp. 566–580

[12] Xu, S., Peng, H., Tang, Y.: 'Preview Path Tracking Control With Delay Compensation for Autonomous Vehicles', *IEEE Trans. Intell. Transp. Syst.*, 2020, pp. 1–11

[13] Pérez, J., Milanés, V., Onieva, E.: 'Cascade architecture for lateral control in autonomous vehicles', *IEEE Trans. Intell. Transp. Syst.*, 2011, **12**, (1), pp. 73–82

[14] Onieva, E., Naranjo, J. E., Milanés, V., Alonso, J., García, R., Pérez, J.: 'Automatic lateral control for unmanned vehicles via genetic algorithms', *Appl. Soft Comput.*, **11**, (1), pp. 1303–1309

[15] Nguyen, A. T., Sentouh, C., Popieul, J. C.: 'Fuzzy steering control for autonomous vehicles under actuator saturation: Design and experiments', *J. Franklin Inst.*, 2018, **355**, (18), pp. 9374–9395

[16] Tan, H. S., Huang, J.: 'Design of a high-performance automatic steering controller for bus revenue service based on how drivers steer', *IEEE Trans. Robot.*, 2014, **30**, (5), pp. 1137–1147

[17] Mohammadpour, J. and Scherer, C. W.: '*Control of linear parameter varying systems with applications*' (Springer Press, Boston, 2012)

[18] Barker, J. M., Balas, G. J.: 'Comparing linear parameter-varying gain-scheduled control techniques for active flutter suppression', *J. Guid. Control Dyn.*, 2000, **23**, (5), pp. 948–955

[19] Sename, O., Gaspar, P., Bokor, J.: '*Robust control and linear parameter varying approaches: Application to vehicle dynamics*' (Springer Press, Berlin, 2013)

[20] Gáspár, P., Szabó, Z., Bokor, J., Nemeth, B.: '*Robust control design for active driver assistance systems*' (Springer Press, Cham, 2012)

[21] Sename, O., Dugard, L., Gaspar, P.: 'H_∞/LPV controller design for an active anti-roll bar system of heavy vehicles using parameter dependent weighting functions', *Heliyon*, 2019, **5**, (6), pp. e01827

[22] Hoffmann, C., Werner, H.: 'A Survey of Linear Parameter-Varying Control Applications Validated by Experiments or High-Fidelity Simulations', *IEEE Trans. Control Syst. Technol.*, 2015, **23**, (2), pp. 416–433

[23] Hingwe, P., Tan, H. S., Packard, A. K., Tomizuka, M.: 'Linear parameter varying controller for automated lane guidance: experimental study on tractor-trailers', *IEEE Trans. Control Syst. Technol.*, 2002, **10**, (6), pp. 793–806

[24] Kang, C. M., Lee, S. H., Chung, C. C.: 'Linear Parameter Varying Design for Lateral Control using Kinematics of Vehicle Motion', Proc. IEEE American Control Conf., Milwaukee, USA, June 2018, pp. 3239–3244

[25] Alcalá, E., Puig, V., Quevedo, J.: 'LPV-MP planning for autonomous racing vehicles considering obstacles', *Rob. Auton. Syst.*, 2020, **124**, pp. 103392

[26] Rajamani, R.: '*Vehicle Dynamics and Control*' (Science Press, Boston, 2011)

[27] Taylor, C. J., Košecká, J., Blasi, R., Malik, J.: 'A comparative study of vision-based lateral control strategies for autonomous highway driving', *Int. J. Rob. Res.*, 1999, **18**, (5), pp. 442–453

[28] Apkarian, P., Gahinet, P., Becker, G.: 'Self-scheduled H_∞ control of linear parameter-varying systems: a design example', *Automatica*, 1995, **31**, (9), pp. 1251–1261

[29] Wu, F.: 'Control of Linear Parameter Varying Systems', PhD Thesis, University of California, Berkeley, 1995

[30] Wu, F., Yang, X. H., Packard, A., Becker, G.: 'Induced L_2-norm control for LPV systems with bounded parameter variation rates', *Int. J. Robust Nonlinear Control*, 1996, **6**, (9-10), pp. 983–998
[31] Becker, G., Packard, A.: 'Robust performance of linear parametrically varying systems using parametrically-dependent linear feedback', *Syst. Control Lett.*, 1994, **23**, (3), pp. 205–215
[32] Coulter, R. C.: 'Implementation of the pure pursuit path tracking algorithm', (Carnegie-Mellon UNIV Pittsburgh PA Robotics INST, 1992)
[33] Hjartarson, A., Seiler, P., Packard, A.: 'LPVTools: A toolbox for modeling, analysis, and synthesis of parameter varying control systems', Proc. IFAC-PapersOnLine Grenoble, France, October 2015, pp. 139–145
[34] Lofberg, J.: 'YALMIP: A toolbox for modeling and optimization in MATLAB.', Proc. IEEE Int. Conf. Robot. Autom., New Orleans, USA, September 2004, pp. 284–289